forum acusticum 2026
8-12 September · Graz, Austria

FROM TRANSMISSION-LINE MODELS TO STUART–LANDAU OSCILLATORS: A HOPF-BASED DESCRIPTION OF COCHLEAR DYNAMICS

Sebastian Handel[1], Martin Hagmüller[1], Gernot Kubin[1]

[1]*Signal Processing and Speech Communication Laboratory, Graz University of Technology, Austria*

This paper is a revised version of the authors' submitted manuscript that was peer-reviewed by at least two anonymous reviewers.

Abstract

Over the past decades, numerous models of the cochlear partition have been proposed to explain key features of cochlear mechanics, including traveling-waves, nonlinear amplification, and compressive responses. Among them, the transmission-line model introduced by George Zweig and extended by others represents the cochlea as a distributed system of coupled resonant elements interacting through the cochlear fluid and successfully reproduces the spatiotemporal dynamics of the basilar membrane.

Another widely used framework describes active auditory processes as nonlinear oscillators operating near a Hopf bifurcation. The Stuart–Landau oscillator (SLO), the normal form of a Hopf bifurcation, captures essential properties such as self-sustained oscillations, nonlinear amplification, and compressive responses, and has therefore been widely used to model active hair-cell dynamics and cochlear amplification.

In this study, we analytically demonstrate that the local dynamics of the transmission-line model admit a Hopf bifurcation and therefore can be reduced to the Hopf normal form. We further show that this reduced oscillator representation describes the local dynamics near the bifurcation. To illustrate the implications of this correspondence, we simulate basilar membrane displacement using an ensemble of coupled SLOs, demonstrating that the reduced oscillator framework reproduces qualitative cochlear features including frequency selectivity, nonlinear compression, half-octave shift, and traveling-wave-like behavior.

Keywords: *Transmission-line model, Stuart-Landau Oscillator, Traveling-wave, Hopf Bifurcation, Center Manifold Reduction, Cochlear Partition Model*

Corresponding author: *sebastian.handel@tugraz.at*

1. Introduction

The mammalian cochlea performs a remarkable mechanical signal-processing task, transforming sound-induced pressure waves into frequency-selective neural responses. Incoming acoustic stimuli generate pressure differences across the cochlear partition that propagate as traveling-waves along the basilar membrane. The resulting vibrations are shaped by the complex micromechanics of the organ of Corti, where the basilar membrane, tectorial membrane, and hair cells interact to produce the characteristic frequency tuning and nonlinear response of the auditory system. These dynamics are not purely passive; instead, they involve an active amplification mechanism, primarily mediated by outer hair cells, that enhances sensitivity to weak stimuli and produces the compressive nonlinearities observed in cochlear responses [1], [2].

To describe the propagation of mechanical waves in the cochlea, several mathematical and computational models have been proposed. One influential class of models represents the cochlea as a transmission line, in which the basilar membrane and organ of Corti are modeled as spatially distributed mechanical impedances coupled through the cochlear fluid. Building on the long history of transmission-line cochlear models, the formulations of Zweig [3] and later Shera [4] formulated the cochlea as a distributed system of coupled resonant elements described as a delay differential equation (DDE) whose interaction with the cochlear fluid produces the traveling-wave-like behavior observed experimentally. In this framework, the inertia of the cochlear fluid provides longitudinal coupling between adjacent elements. At the same time, the local mechanical impedance determines the frequency-dependent response of each section of the cochlear partition. Transmission-line models have proven highly successful in reproducing key features of cochlear mechanics, including the spatial progression of the traveling-wave and the frequency-dependent tuning along the basilar membrane [5].

More recent work has extended this framework to incorporate the cochlea's active nonlinear mechanics. In particular, models developed by Verhulst and collaborators [6], [7] introduced an important modification to the classical transmission-line formulation by allowing the poles of the local mechanical transfer function to shift with instantaneous amplitude. Earlier transmission-line models were largely linear systems with fixed pole locations determining the resonance characteristics of each cochlear partition element. In contrast, the model from [4] introduces instantaneous amplitude dependent pole shifting, effectively modeling the cochlear amplifier and generating compressive nonlinear responses consistent with experimental observations. In this formulation, each longitudinal section of the cochlea is represented by a local filter whose pole locations determine the basilar-membrane response's resonance frequency and damping. Allowing these poles to move in the complex plane as a function of instantaneous amplitude provides a computationally efficient mechanism for incorporating active cochlear amplification into the transmission-line framework while preserving the traveling-wave propagation along the basilar membrane.
An alternative theoretical perspective frames cochlear amplification as a nonlinear dynamical system operating near a Hopf bifurcation. In this framework, the active elements of the cochlea are assumed to operate near a dynamical instability. Near such a bifurcation, the dynamics can be described by the SLO, which represents the normal form of the Hopf bifurcation. This model has been derived from a damped spring–mass system by Vilfan and Duke [8] and has been successfully compared to spontaneous otoacoustic emissions (SOAEs) observed in lizards. More generally, Hopf-type oscillator models have been widely used to describe the active mechanics of hair bundles and outer hair cells, and to explain key phenomena such as sharp frequency tuning and SOAEs [9], [10], [11].
Although transmission-line and oscillator-based cochlear models are often treated as separate frameworks, Ver Hulst et al. [12] showed that the local dynamics underlying Zweig's cochlear model are mathematically equivalent to the linearized dynamics of an active oscillator near a Hopf bifurcation. In this view, the instantaneous amplitude dependent pole shifting introduced can be interpreted as a reduction of effective damping that brings the system closer to dynamical instability, motivating a nonlinear systems analysis of the model.
Motivated by these considerations, the present study investigates the dynamical properties of the transmission-line model. We show that its local dynamics possess a Hopf bifurcation and can therefore be reduced to the Hopf normal form. This establishes a direct connection between the local transmission-line dynamics and SLO description of cochlear amplification, providing a simplified dynamical representation that preserves key features such as frequency selectivity, nonlinear compression, half-octave shift and traveling-wave-like behavior. To illustrate the implications of this correspondence, an ensemble of coupled SLOs is simulated to investigate whether the reduced oscillator framework reproduces qualitative cochlear features.

2. Derivation of the Hopf Normal Form

A local isolated element of the transmission-line model proposed by [7] can be described by a DDE [13]. The model describes the displacement x and velocity v of the cochlear partition at a given longitudinal position. It is formulated as a damped spring–mass system with mass m, stiffness k, damping d, and a nonlinear delayed feedback term of the form $\Psi(x(t-\tau))x(t-\tau)$, where Ψ is the active OHC feedback gain and $\Psi(x(t-\tau)) \geq 0$ with $\tau \in \mathbb{R}$.

$$\begin{aligned} \dot{x} &= v \\ \dot{v} &= -\frac{k}{m}x - \frac{d}{m}v - \frac{1}{m}\Psi(x(t-\tau))x(t-\tau). \end{aligned} \quad (1)$$

Define the natural frequency $\tilde{\omega}_0$,the normalized damping $\tilde{\mu}$, and the delayed displacement x_τ

$$\begin{aligned} \tilde{\omega}_0 &= \sqrt{\frac{k}{m}}, \\ \tilde{\mu} &= \frac{d}{m}, \\ x_\tau &= x(t-\tau). \end{aligned} \quad (2)$$

Then

$$\dot{v} = -\tilde{\omega}_0^2 x - \tilde{\mu}v - \frac{1}{m}\Psi(x_\tau)x_\tau. \quad (3)$$

The equilibrium is

$$\begin{aligned} \dot{x} &= 0, \\ \dot{v} &= 0. \end{aligned} \quad (4)$$

The nonlinear function Ψ is expanded as

$$\begin{aligned} \dot{v} &= -\tilde{\omega}_0^2 x - \tilde{\mu}v \\ &-\frac{1}{m}\left(\Psi(0)x_\tau + \Psi'(0)x_\tau^2 + \Psi''(0)\frac{x_\tau^3}{2}\right). \end{aligned} \quad (5)$$

In the following sections, it is shown that this system can be reduced near a Hopf bifurcation to the normal form

$$\dot{z} = (\mu + j\omega_0)z - (\alpha + j\beta)|z|^2 z, \quad (6)$$

where μ denotes the effective linear damping parameter, ω_0 the natural frequency of the linearized system, and α and β the nonlinear damping and nonlinear frequency shift coefficients, respectively.

2.1. Hopf Conditions

For DDEs, solutions of the linearized system are of the form $Ae^{\lambda t}$ with characteristic roots (roots)

$$\lambda = \sigma + j\Omega. \quad (7)$$

A Hopf bifurcation occurs when the trajectory of a pair of complex conjugate eigenvalues in the complex plane crosses the imaginary axis as a system parame-

ter is varied. For this to occur, two conditions must be satisfied [13].
The first condition requires that, at the bifurcation point, the roots with the largest real part are purely imaginary:

$$H_1 : \max \quad \Re(\lambda) \Rightarrow \lambda_0 = \pm j\Omega. \tag{8}$$

The second condition ensures that the real part of the roots changes sign as the parameter passes through the bifurcation point $\tilde{\mu}_0$:

$$H_2 : \Re\left(\frac{\partial \lambda}{\partial \tilde{\mu}}(\tilde{\mu}_0)\right) \neq 0. \tag{9}$$

For the analysis, we use the exponential ansatz.

$$\begin{aligned} x(t) &= Ae^{\lambda t} \\ v(t) &= A\lambda e^{\lambda t} \\ \dot{v}(t) &= A\lambda^2 e^{\lambda t}. \end{aligned} \tag{10}$$

2.1.1. Condition H_1
Linearizing around the equilibrium and substituting the exponential ansatz yields the characteristic equation, whose roots determine the system's stability. Since the system is a DDE, it possesses infinitely many characteristic roots. However, at this stage of the Hopf bifurcation analysis, only roots on the imaginary axis are considered.

$$h(\lambda) = -\lambda^2 - \tilde{\omega}_0^2 - \tilde{\mu}\lambda - \frac{\Psi(0)}{m}e^{-\lambda\tau} = 0. \tag{11}$$

At the Hopf bifurcation, separating real and imaginary parts gives

$$-\frac{\Psi(0)}{m}\cos(\tilde{\omega}_0\tau) = 0 \tag{12}$$

$$\tilde{\mu}_0\tilde{\omega}_0 + \frac{\Psi(0)}{m}\sin(\tilde{\omega}_0\tau) = 0. \tag{13}$$

Hence, Eq. (12),

$$\cos(\tilde{\omega}_0\tau) = 0, \tag{14}$$

which implies $\tilde{\omega}_0\tau = \frac{\pi}{2} + k\pi, \quad k \in \mathbb{Z}$. The corresponding parameter value for $\tilde{\mu}$ is found from Eq. (13)

$$\tilde{\mu}_0 = -\frac{\Psi(0)}{m\tilde{\omega}_0}\sin(\tilde{\omega}_0\tau). \tag{15}$$

Choosing the branch

$$\tau = \tau_0 = \frac{\pi}{2\tilde{\omega}_0} \tag{16}$$

yields

$$\tilde{\mu}_0 = -\frac{\Psi(0)}{m\tilde{\omega}_0}. \tag{17}$$

At this point, the roots are $\lambda = \pm j\tilde{\omega}_0$. The characteristic roots depend continuously on τ. At $\tau = 0$, all roots satisfy $\Re(\lambda) < 0$ since

$$\lambda = \frac{\tilde{\mu}_0 \pm \sqrt{\tilde{\mu}_0^2 - 4\left(\tilde{\omega}_0^2 + \frac{\Psi(0)}{m}\right)}}{2}, \tag{18}$$

and therefore

$$\sigma_{\tau=0} = \frac{\tilde{\mu}_0}{2} < 0. \tag{19}$$

By continuity of the roots with respect to τ, and since only one simple pair reaches the imaginary axis, all remaining roots satisfy $\Re(\lambda) < 0$ at τ_0. Hence, H1 holds.

2.1.2. Condition H_2
The roots satisfy

$$h(\lambda(\tilde{\mu}), \tilde{\mu}) = 0. \tag{20}$$

Differentiating with respect to $\tilde{\mu}$ yields

$$\frac{\partial h}{\partial \tilde{\mu}} = \frac{\partial h}{\partial \lambda}\frac{\partial \lambda}{\partial \tilde{\mu}} + \frac{\partial h}{\partial \tilde{\mu}} = 0, \tag{21}$$

so that

$$\frac{\partial \lambda}{\partial \tilde{\mu}} = -\frac{\lambda}{-2\lambda - \tilde{\mu} + \tau_0\frac{\Psi(0)}{m}e^{-\lambda\tau_0}}. \tag{22}$$

Evaluating at $\lambda = j\tilde{\omega}_0$ gives

$$\frac{\partial \lambda}{\partial \tilde{\mu}}(\tilde{\mu}_0) = \frac{-j\tilde{\omega}_0}{\tilde{\mu}_0 - j\left(2\tilde{\omega}_0 + \tau_0\frac{\Psi(0)}{m}\right)}. \tag{23}$$

If $\tilde{\omega}_0 \neq 0$ and $2\tilde{\omega}_0 + \tau_0\frac{\Psi(0)}{m}) \neq 0$, it follows that

$$\Re\left(\frac{d\lambda}{d\tilde{\mu}}(\tilde{\mu}_0)\right) \neq 0. \tag{24}$$

Thus, condition H_2 is satisfied.
This shows that the system has a Hopf bifurcation at $\tau = \frac{\pi}{2\tilde{\omega}_0}$ and $\tilde{\mu} = \frac{\Psi(0)}{m\tilde{\omega}_0}$.

2.2. Center Manifold Reduction

Near the bifurcation, only the critical eigenmodes contribute to the dynamics, as all other modes decay exponentially and are therefore slaved to the critical modes (as shown in Section 2.1.1). Consequently, the system can be reduced to a two-dimensional center eigenspace. The solution can therefore be written as

$$\begin{aligned} x &= A\left(e^{j\tilde{\omega}_0 t} + e^{-j\tilde{\omega}_0 t}\right) \\ v &= j\tilde{\omega}_0 A\left(e^{j\tilde{\omega}_0 t} - e^{-j\tilde{\omega}_0 t}\right) \end{aligned} \tag{25}$$

which can be a complex variable

$$z = x - \frac{j}{\tilde{\omega}_0}v. \tag{26}$$

Substituting into the nonlinear equation yields

$$\begin{aligned} \dot{z} - \dot{\overline{z}} = &\left(j\tilde{\omega}_0 - \tilde{\mu} + j\frac{\Psi(0)}{m\tilde{\omega}_0}e^{j\tilde{\omega}_0\tau}\right)z \\ &+\left(j\tilde{\omega}_0 + \tilde{\mu} + j\frac{\Psi(0)}{m\tilde{\omega}_0}e^{j\tilde{\omega}_0\tau}\right)\overline{z} \\ &+\frac{\Psi'(0)}{m\tilde{\omega}_0}\left(z_\tau^2 + 2z_\tau\overline{z}_\tau + \overline{z}_\tau^2\right) \\ &+\frac{\Psi''(0)}{2\tilde{\omega}_0 m}\left(z_\tau^3 + 3z_\tau^2\overline{z}_\tau + 3z_\tau\overline{z}_\tau^2 + \overline{z}_\tau^3\right). \end{aligned} \tag{27}$$

Only resonant terms that match the critical eigenfrequency contribute to the reduced dynamics, while non-resonant terms are absorbed into higher-order correction terms. Projecting onto the center eigenspace yields

$$\dot{z} = \left(-\tilde{\mu} + j\tilde{\omega}_0 + j\frac{\Psi(0)}{m\tilde{\omega}_0}e^{-j\tilde{\omega}_0\tau}\right)z + \frac{3}{2\tilde{\omega}_0 m}\Psi''(0)e^{-j\tilde{\omega}_0\tau}|z|^2 z. \tag{28}$$

Introduce the coefficients

$$\begin{aligned}\tilde{\mu}_\Psi + j\tilde{\omega}_{0_\Psi} &= j\frac{\Psi(0)}{m\tilde{\omega}_0}e^{-j\tilde{\omega}_0\tau}\\ -\alpha - j\beta &= \frac{3}{2\tilde{\omega}_0 m}\Psi''(0)e^{-j\tilde{\omega}_0\tau}.\end{aligned} \tag{29}$$

The Hopf normal form becomes

$$\dot{z} = (\mu + j\omega_0)z - (\alpha + j\beta)|z|^2 z. \tag{30}$$

with the parameter

$$\begin{aligned}\mu &= \tilde{\mu}_\Psi - \tilde{\mu}\\ \omega_0 &= \tilde{\omega}_0 + \omega_\Psi\end{aligned} \tag{31}$$

Evaluating at the bifurcation point yields

$$\dot{z} = (j\omega_0)z - \left(j\frac{3}{2\omega_0 m}\Psi''(0)\right)|z|^2 z, \tag{32}$$

which is consistent with the normal form at the Hopf bifurcation. This shows that a local isolated element of the transmission-line model reduces to an SLO in a neighborhood of the bifurcation. Although the local dynamics reduce to a Stuart–Landau oscillator near the bifurcation, transmission-line models remain spatially distributed systems. Therefore, nearest-neighbor coupling is introduced in Eq. (33) as a phenomenological approximation of the interactions between neighboring cochlear partitions.

2.3. Numerical Simulation of Stuart–Landau Oscillators

The oscillator dynamics derived in the previous section are simulated numerically using ensembles of SLOs. To allow both deterministic and stochastic simulations within the same framework, the system is formulated as a stochastic differential equation (SDE). The general form used in the simulations is

$$\begin{aligned}\dot{z}_i = (\mu_i + i\omega_{0,i})z_i - (1 + i\beta_i)|z_i|^2 z_i\\ + C_i(z) + \nu_i(t) + F(t).\end{aligned} \tag{33}$$

Here $z_{i(t)}$ denotes the complex oscillator state and μ, ω_i, and β are the parameters introduced previously. The term α is always set to 1 because its influence can be modeled by μ [14]. The term $\nu_{i(t)}$ represents a stochastic contribution modeled as a Wiener process, while $C_{i(z)}$ and $F(t)$ denote coupling and external forcing terms.

Formulating the system as a stochastic differential equation allows stochastic perturbations to be included in the oscillator dynamics when required. The stochastic term $\nu_{i(t)}$ can be used to introduce white-noise fluctuations acting on the oscillator state. When this term is disabled, the system reduces to a deterministic ordinary differential equation. In this way, deterministic and stochastic simulations can be treated within a unified numerical framework.

Following [15], oscillators are arranged in a one-dimensional chain and coupled to their nearest-neighbors. The coupling is governed by the stiffness and damping coefficients κ and γ, yielding

$$\begin{aligned}C_i(z) = \kappa_{i-1}\Re(z_{i-1}) + \kappa_{i+1}\Re(z_{i+1})\\ + j(\gamma_{i-1}\Im(z_{i-1}) + \gamma_{i+1}\Im(z_{i+1})).\end{aligned} \tag{34}$$

Coupling-induced perturbations motivate the SDE formulation. Simulations are implemented in Julia using DifferentialEquations.jl and a Stability-Optimized Stochastic Runge–Kutta method, with interpolated input signals and initial conditions obtained from an unforced simulation. The simulation code and a more detailed explanation are available in our GitHub repository. Earcillator.

3. Results

To demonstrate the model's capability to reproduce cochlear partition responses, a simulation was performed using an ensemble of 600 SLOs, logarithmically spaced between 200Hz and 16kHz, according to the frequency-place map proposed by Greenwood [16]. The oscillators were coupled via nearest-neighbor interactions, and no stochastic noise was included. To account for the amplification of the outer and middle ear, the input signal was amplified by 20dB.

It should be noted that the last 50 oscillators (between 8192Hz and 16kHz) did not reach a steady-state response within the simulation time. This behavior was observed independently of the specific choice of characteristic frequencies and is likely due to coupling-induced boundary effects, leading to altered dynamics at the ends of the oscillator array compared to its central region. Therefore, the responses of these oscillators were excluded from the following analysis. Nevertheless, this phenomenon is of potential interest and warrants further investigation, although it is beyond the scope of this work.

In Figure 1, the steady-state response of the oscillator ensemble to sinusoidal stimuli at 1kHz with varying SPL is shown. The results exhibit pronounced frequency selectivity at low input levels (e.g., from 10dB to 50dB SPL), which decreases with increasing stimulus amplitude. In addition, the peak response shifts toward higher characteristic frequencies as the input level increases. Furthermore, a clear compressive nonlinearity is observed for input levels above approximately 50dB SPL.

In Figure 2, the displacement of a subset of the oscillator ensemble prior to steady-state is shown. The results illustrate the propagation of a traveling-wave along the oscillator array, with the response peak moving from basal (high-frequency) to apical (low-frequency) regions over time. The amplitude evolves along the array, reaching its maximum near the oscillator whose characteristic frequency is closest to the stimulus frequency.

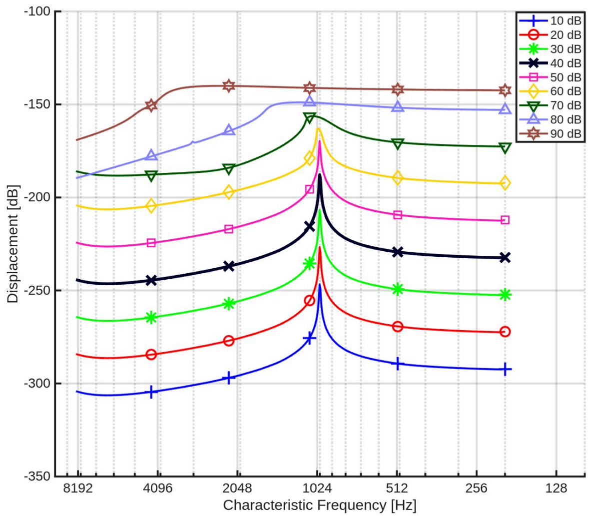

Figure 1: RMS displacement of 550 SLOs in the ensemble with nearest-neighbor coupling for a 1kHz sinusoidal stimulus at different SPLs, evaluated over 250 ms of steady state. Parameters: $\mu_i = 0$, $\beta_i = 1$, $k = 5$, $d = 5$, no noise, 600 oscillators logarithmically spaced between 200 Hz and 16 kHz.

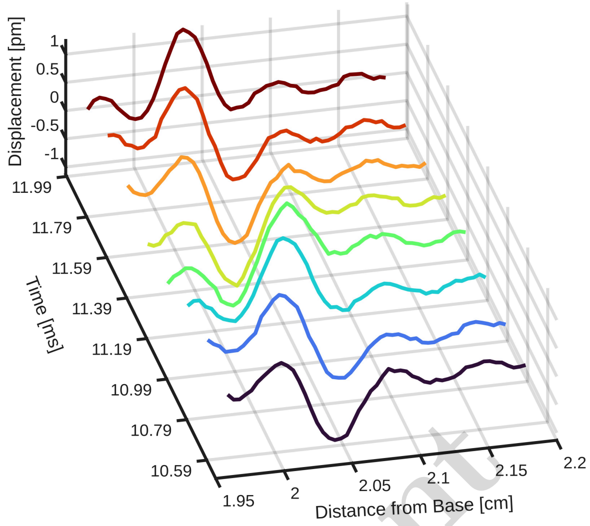

Figure 2: Displacement of 51 SLOs in the ensemble with nearest-neighbor coupling for a 1 kHz sinusoidal stimulus at 20 dB SPL before reaching steady state. Parameters: $\mu_i = 0$, $\beta_i = 1$, $k = 5$, $d = 5$, no noise. Each color in the representation corresponds to a specific point in time. A video of the traveling-wave is available at Earcillator

4. Discussion

The derivation shows that an SLO can locally approximate the transmission-line model near a Hopf bifurcation, as delayed feedback introduces an effective velocity-dependent term. For oscillations near the characteristic frequency ($\omega\tau \approx \frac{\pi}{2}$), the delayed displacement is proportional to

$$x(t-\tau) \propto -v(t), \tag{35}$$

so that the feedback force

$$F_{fb} = -\frac{\Psi(x(t-\tau))}{m} x(t-\tau) \tag{36}$$

becomes proportional to $+v(t)$. This corresponds to negative damping, i.e., a force acting in phase with the velocity, which injects energy into the system and leads to amplification. This mechanism is consistent with classical descriptions of self-oscillatory systems [17].

This interpretation also aligns with the physiological description of cochlear mechanics by Lukashin et al. [18], in which OHCs and the tectorial membrane provide active feedback to the basilar membrane. When the stimulus frequency matches the characteristic frequency, the system naturally operates close to the required phase condition, resulting in amplification. This suggests that an SLO can effectively describe a local cochlear partition near the bifurcation.

The functional form of Ψ plays a crucial role, as it determines whether the system exhibits unbounded growth or saturates at a finite amplitude. As discussed by Ashmore [19], the transfer function between hair-bundle displacement and receptor potential of outer hair cells can be described by a monotonically decreasing sigmoidal function. If Ψ follows a bounded decreasing function, the effective feedback strength decreases with increasing displacement, which prevents unbounded growth and leads to a stable oscillatory response.

As illustrated in Figure 1, the model reproduces key cochlear features, including sharp frequency selectivity at low amplitudes, a shift of the peak response toward higher frequencies at higher amplitudes, and nonlinear compression. These characteristics are consistent with results from transmission-line models [6] (Figure 2C) and experimental observations in the mammalian cochlea [2].

Furthermore, Figure 2 demonstrates that an ensemble of coupled SLOs can reproduce a traveling-wave-like pattern. Importantly, this wave does not arise from a propagation of the stimulus through the chain of coupled oscillators.

Instead, all oscillators are driven, and the apparent traveling-wave emerges from differences in phase and amplitude across the ensemble. Each oscillator responds with its own phase delay and gain, resulting in a temporal-spatial pattern corresponding to a traveling-wave. Similar entrainment-induced wave patterns have been reported for coupled nonlinear oscillators such as the van der Pol system [20].

The transmission-line model, due to its delay term, is inherently infinite-dimensional and can exhibit complex dynamical behavior, including chaos. In contrast, the reduced Stuart–Landau description is effectively two-dimensional near the Hopf bifurcation and captures the system's dominant deterministic dynamics. However, a deterministic two-dimensional system cannot exhibit chaos. Intrinsic noise can induce chaotic dynamics in the reduced model [21], allowing it to capture complex dynamics otherwise associated with higher-dimensional systems such as the transmission-line model.

5. Conclusion

This work shows that the local delayed dynamics underlying the considered transmission-line formulation admit a Stuart–Landau oscillator description near a Hopf bifurcation. The reduction replaces the original DDE with a significantly simpler ODE or SDE while preserving qualitative features such as frequency selectivity and nonlinear compression.

Furthermore, an ensemble of coupled SLOs offers an abstract yet insightful representation of cochlear partition dynamics. Interpreting the cochlea as a tonotopically organized array of coupled oscillators explains how spatially distributed phase and amplitude differences can give rise to traveling-wave-like behavior through entrainment, even when all oscillators are driven simultaneously.

At the same time, the nearest-neighbor coupling used in the model leads to distinct behavior at the boundaries of the oscillator ensemble. This raises the question of whether similar edge effects occur in the biological cochlea, and if not, which structural or dynamical mechanisms prevent them.

Finally, the reduction from an infinite-dimensional transmission-line model to a two-dimensional system suppresses potentially chaotic dynamics that a deterministic SLO cannot exhibit on its own. Such dynamics may be reintroduced through noise, coupling, or external perturbations, motivating the use of SDE models.

5.1. Author contributions

S.H.: Conceptualization, Methodology, Formal analysis, Software, Visualization, Writing – original draft.
M.H.: Conceptualization, Validation, Writing – Review & Editing, Supervision.
G.K.: Conceptualization, Validation, Writing – Review & Editing, Supervision.

References

[1] A. Hudspeth, "Making an effort to listen: Mechanical amplification in the ear," *Neuron*, vol. 59, no. 4, pp. 530–545, 2008.

[2] C. J. Plack, *The sense of hearing*. Routledge, 2023.

[3] G. Zweig, "Finding the impedance of the organ of Corti," *The Journal of the Acoustical Society of America*, vol. 89, no. 3, pp. 1229–1254, 1991.

[4] C. A. Shera, "Intensity-invariance of fine time structure in basilar-membrane click responses: Implications for cochlear mechanics," *The Journal of the Acoustical Society of America*, vol. 110, no. 1, pp. 332–348, 2001.

[5] G. Ni, S. J. Elliott, M. Ayat, and P. D. Teal, "Modelling cochlear mechanics," *BioMed Research International*, vol. 2014, no. 1, p. 150637, 2014.

[6] S. Verhulst, T. Dau, and C. A. Shera, "Nonlinear time-domain cochlear model for transient stimulation and human otoacoustic emission," *The Journal of the Acoustical Society of America*, vol. 132, no. 6, pp. 3842–3848, 2012.

[7] S. Verhulst, A. Altoe, and V. Vasilkov, "Computational modeling of the human auditory periphery: Auditory-nerve responses, evoked potentials and hearing loss," *Hearing Research*, vol. 360, pp. 55–75, 2018.

[8] A. Vilfan and T. Duke, "Frequency clustering in spontaneous otoacoustic emissions from a lizard's ear," *Biophysical Journal*, vol. 95, no. 10, pp. 4622–4630, 2008.

[9] S. Camalet, T. Duke, F. Jülicher, and J. Prost, "Auditory sensitivity provided by self-tuned critical oscillations of hair cells," *Proceedings of the National Academy of Sciences*, vol. 97, no. 7, pp. 3183–3188, 2000.

[10] V. M. Eguíluz, M. Ospeck, Y. Choe, A. Hudspeth, and M. O. Magnasco, "Essential nonlinearities in hearing," *Physical Review Letters*, vol. 84, no. 22, p. 5232, 2000.

[11] A. Hudspeth, F. Jülicher, and P. Martin, "A critique of the critical cochlea: Hopf—a bifurcation —is better than none," *Journal of Neurophysiology*, vol. 104, no. 3, pp. 1219–1229, 2010.

[12] H. Ver Hulst, C. B. Mercader, F. Jülicher, and P. Martin, "Marrying critical oscillators with traveling waves shapes nonlinear sound processing in the cochlea," *arXiv preprint arXiv:2512.11646*, 2025.

[13] J. K. Hale and S. M. V. Lunel, *Introduction to Functional Differential Equations*, vol. 99. Springer Science & Business Media, 2013.

[14] J. Faber and D. Bozovic, "Criticality and chaos in auditory and vestibular sensing," *Scientific Reports*, vol. 14, no. 1, p. 13073, 2024.

[15] B. Epp and M. B. Rasmussen, "Entrainment effects and information processing in coupled oscillator models of auditory biomechanics," *bioRxiv*, pp. 2025–2029, 2025.

[16] D. D. Greenwood, "Critical bandwidth and the frequency coordinates of the basilar membrane," *The Journal of the Acoustical Society of America*, vol. 33, no. 10, pp. 1344–1356, 1961.

[17] A. Jenkins, "Self-oscillation," *Physics Reports*, vol. 525, no. 2, pp. 167–222, 2013.

[18] A. N. Lukashkin, G. P. Richardson, and I. J. Russell, "Multiple roles for the tectorial membrane in the active cochlea," *Hearing research*, vol. 266, no. 1–2, pp. 26–35, 2010.

[19] J. Ashmore, "Cochlear outer hair cell motility," *Physiological reviews*, vol. 88, no. 1, pp. 173–210, 2008.

[20] L. M. Sørensen, P. L. Bysted, and B. Epp, *Clustering in an array of nonlinear and active oscillators as a model of spontaneous otoacoustic emissions*. Universitätsbibliothek der RWTH Aachen, 2019.

[21] J. Faber and D. Bozovic, "Chaotic dynamics enhance the sensitivity of inner ear hair cells," *Scientific reports*, vol. 9, no. 1, p. 18394, 2019.